1

The Synthesis, Properties, and Biological Action of Metal Complexes with Schiff Bases

DR J NIJALINGAPPA[1], DR K SHARANABASSAMMA[2]

Assoc. Professor[1], Professor2

niji.jrashi@gmail.com , sharanabenni.k@gmail.com

Department of Chemistry, Proudhadevaraya Institute of Technology, Abheraj Baldota Rd, Indiranagar,

Hosapete, Karnataka-583225

Abstract:

The following metal complexes of Schiff bases have been reported and characterised: 2-furancarboxaldehyde and o-phenylenediamine (L1), and 2-thiophenecarboxaldehyde and 2-aminothiophenol (HL2). The analyses were conducted using thermal analysis (TGA), elemental analyses, infrared 1H NMR, solid reflectance, magnetic moment, and chemical analysis. The pH-metric calculation of the ligand dissociation and metal-ligand stability constants was performed at 25 °C and an ionic strength of $\mu = 0.1$ (1 M NaCl). A number of complexes with the formula $[M(L1)(H2O)2]$ have been identified.With M = Fe(III), Ni(II), Cu(II), n = 2-3, and y = 2-4, the equation becomes (Cl)n·yH2 O) [M(L1)].X squaredWhere M is Co(II), Zn(II), or UO2(II), X is Cl, AcO, or NO3, and y ranges from 1 to 3, M(L2)2 is the equation to be used.In the above equation, M may be represented by Co(II), Ni(II), or Cu(II); X can be Cl, y can be between 0 and 2; and Zn(II) can be represented by AcO, y can be zero; and $[Fe(L2)2]Cl·2H2O$ and $[UO2(HL2)2](NO3)2$. According to the molar conductance data, the HL2 chelates of Co(II), Ni(II), Cu(II), and Zn(II) are not electrolytes, but the HL2 chelates of Fe(III) and UO2(II) are. Using infrared spectra, we can see that L1 has a tetradentate coordination to the metal ions via the ONNO donor sites of azomethine-N and furan-O, and that HL2 has a terdentate coordination through the SNS donor sites of azomethine-N, thiophene-S, and thiol-S. Octahedral and tetrahedral geometrical structures are determined from the magnetic and solid reflectance spectra of these complexes. According to the chelates' thermal behaviour, the hydrated complexes undergo hydration-related molecular loss in the first stage, followed by the decomposition of anions and ligand molecules in the following phases. E^*, ΔH^*, ΔS^*, and ΔG^* are activation thermodynamic parameters that are computed from the DrTG curves by using the Coats-Redfern technique. Antibacterial activity against bacterial species, Pseudomonas aeruginosa, Staphylococcus Pyogones, and fungi (Candida) was also tested for in the synthesised ligands compared to their metal complexes. The activity findings demonstrate that the metal complexes exhibit superior antibacterial properties compared to the parent Schiff base ligand against at least one bacterium species.

Introduction

A large number of Schiff bases and their complexes have been studied for their interesting and important properties, e.g., their ability to reversibly bind oxygen[1], catalytic activity in hydrogenation of olefins[2] and transfer of an amino group[3], photochromic properties[4], and complexing ability towards some toxic metals[5]. The high affinity for the chelation of the Schiff bases towards the transition metal ions is utilized in preparing their solid complexes.

Schiff base derived from the reaction of 2,5-thiophenedicarboxaldehyde and o-amino-benzenethiol gives 2,5-bis(benzothiazolidin-2-yl)thiophene(I). Schiff base reacted as a neutral ligand with Pb(II) and a dianion with Cu(II), Ag(I), Cd(II), Pb(II), and Zn(II). The behavior of (I) with Hg(II), Ru(II), Pt(II), Rh(III), and Ni(II) involved the opening of the thiazoline rings of the ligand[6.]

The condensation of o-aminothiophenol with 2-thiophenecarboxaldehyde yields 2-thiazolin-2-ylthiop- hene, rather than the expected Schiff base. However, upon reaction with metal ions, the thiazoline rearranged to the expected thiolate Schiff base. Complexes of Schiff base with Ni(II),Cu(II), Zn(II), Cd(II), Pb(II), Ag(I), and Pd(II) were isolated and characterized[7].

MLL^1 (M = Cu(II), Ni(II); HL = salicylideneamine; HL^1 = 1-(2-hydroxyphenyl)ethyliden-eamine), ML^1L^2(HL^2 = 2-hydroxy-1-naphthylmethyleneamine), and MLL^2reacted with 2-amino-benzenethiol to give Cu_2L^3 ($H_2L^3_2$ = N-(2-mercaptophenyl)salicylaldimine (SMAH), N-(2-mercaptophenyl)-2-hydroxy-1- naph-thylmethyleneamine (NMAH), NiL^3(AMA) (AMAH = N-(2-mercaptophenyl)-1-(2-hydroxyphenyl)ethylide-neamine) and Ni(SMA)(NMA). The complexes were characterized by IR, reflectance spectra, and TGA[8].

Schiff base[9] derived from the reaction of the aldehydes, 3-hydroxybenzaldehyde and

5-nitrosalicylaldehyde, with the amines, aniline and o-aminothiophenol, and their complexes with VO(II), Co(II), and Ni(II), were prepared and characterized by elemental analyses, magnetic measurement, and electronic absorption data.

Complexes of Ni(II), Co(II), Cu(II), Zn(II), Pd(II), and Pb(II) with Schiff base derived from isatin with 2-aminothiophenol (HIATP) were synthesized and characterized by elemental analyses, molar conductance, magnetic moments, ^{1}H NMR, IR, and electronic spectra studies[10].

Spectroscopic investigation of some thio-Schiff bases of 2-aminothiophenol with benzaldehyde deriva- tives has been described[11]. Chemical shifts of the different types of protons in the NMR spectra of the prepared Schiff bases were also reported.

Schiff bases derived from 5-nitrosalicylaldehyde and the amines, o- and p-aminophenols, o-aminothiop-henol, and sulfanilic acid were prepared and their complexes were characterized by IR, electronic absorption, ESR spectra, and magnetic and conductance measurements[12]. The complexes were tested for antibacterial activity against common pathogenic organisms and showed mild to moderate activity.

Schiff bases derived from ethylene-2,2'-(dioxydibenzenaldehyde) and 2-aminothiophenol and its com- plexes with Ni(II), Cu(II), and Cd(II) were synthesized and characterized by elemental analyses, IR, UV/VIS spectra, and conductance measurements[13].

Synthesis, spectroscopic characterization, redox, and biological screening studies of some Schiff bases transition metal(II) complexes derived from salicylidene-4-aminoantipyrine and 2-aminophenol, 2- aminothiophenol were studied by Raman et al.[14].

Schiff bases, 2,5-bis[formyl(2-hydroxyethylamine)]thiophene (H_2L) and 2,5-bis[formyl] (2-mercaptoani-

line)thiophene (H₂L') were prepared and their Cu(II) complexes were also prepared and characterized by elemental analyses, IR, ^{1}H NMR, and conductance and magnetic susceptibility[15].

Experimental

Materials and Reagents

All chemicals used were of analytical reagent grade (AR) and of the highest purity available. They in- cluded 2-thiophenecarboxaldehyde (Sigma), 2-furancarboxaldehyde (Sigma), o-phenylenediamine (Aldrich), 2-aminothiophenol (Sigma), copper(II) acetate dihydrate (Prolabo), cobalt(II) and nickel(II) chloride hex- ahydrates (BDH), zinc acetate dihydrate (Ubichem), uranyl nitrate hexahydrate (Sigma), ferric chloride hexahydrate (Prolabo), zinc oxide, disodium salt of ethylenediaminetetraacetic acid (EDTA) (Analar), am- monia solution (33% v/v), and ammonium chloride (El-Nasr Pharm. Chem. Co., Egypt). The organic solvents used included absolute ethyl alcohol, diethylether, and dimethylformamide (DMF). These solvents were either spectroscopically pure from BDH or purified by the recommended methods[16] and tested for their spectral purity. In addition, hydrogen peroxide, sodium chloride, sodium carbonate, sodium hydrox- ide (A.R.), and hydrochloric and nitric acids (Merck) were used. De-ionized water collected from all-glass equipment was normally used in all preparations.

Solutions

Fresh stock solutions of 1 x 10^{-3}M ligands, L^1 and HL^2, were prepared by dissolving the accurately weighed amount of L^1 (0.264 g/L) and HL^2 (0.219 g/L) in the appropriate volume of absolute ethanol. Then 1 x 10^{-3}M stock solutions of the metal salts (Fe(III), 0.271 g/L; Co(II), 0.238 g/L; Ni(II), 0.238 g/L; Cu(II), 0.218 g/L; Zn(II), 0.219 g/L; UO₂(II), 0.50 g/L) were prepared by dissolving accurately weighed amounts of the metal salts in appropriate volumes of de-ionized water. The metal salt solutions were standardized by the recommended procedures[17]. Dilute solutions of the metal ions and Schiff bases under study of 2.5 x 10^{-6} M, 1 x 10^{-6} M, 2.5 x 10^{-5}M, 1 x 10^{-5} M, and 1 x 10^{-4} M were prepared with accurate dilution.

For potentiometric studies, all solutions of the metal ions were prepared by dissolving the calculated amount of their salts in the least amount of water possible; then ethanol was added to the appropriate volume. Standard 0.1 N sodium carbonate solution was prepared from dried sodium carbonate. 0.10 N hydrochloric acid was prepared and standardized using sodium carbonate. 1.00 M sodium chloride solution was also prepared. A 1:1 sodium hydroxide solution was prepared from A.R. product and stored in a well steamed, waxed tall glass cylinder for several days, with occasional shaking to obtain a carbonate-free sodium hydroxide solution. The clear solution was filtered through a sintered glass funnel (G4). Solutions of required molarity were prepared by dilution and then standardized by the recommended procedure[17].

Instruments

The spectrophotometric measurements in solution were carried out using an automated spectrophotometer UV/VIS Perkin-Elmer Model Lambda 20, and ranged from 200 to 900 nm. pH measurements were per- formed using a Metrohm 716 DMS Titrino connected to a Metrohm 728 Stirrer. The molar conductance of solid complexes in DMF was measured using a Sybron-Barnstead conductometer (Meter-PM.6, E = 3406).

Elemental microanalyses of the separated solid chelates for C, H, N, and S were performed in the Micro- analytical Center, Cairo University. The analyses were repeated twice to check the accuracy of the data. Infrared spectra were recorded on a Perkin-Elmer FT-IR type 1650 spectrophotometer in wavenumber region 4000-200 cm^{-1}. The spectra were recorded as KBr pellets. The solid reflectance spectra were measured on a Shimadzu 3101pc spectrophotometer. The molar magnetic susceptibility was measured on powdered samples using the Faraday method. The diamagnetic corrections were made by Pascal's constant and Hg[Co(SCN)$_4$] was used as the calibrant. The thermogravimetric analysis (TGA and DrTGA) was carried out in a dynamic nitrogen atmosphere (20 mL.min^{-1}), with a heating rate of 10 °C min^{-1} using Shimadzu TGA-50H thermal analyzers. The mass spectra were recorded by the EI technique at 70 eV with a Hewlett-Packard MS-5988 GS-MS instrument in the Microanalytical Center of Cairo University. The ^{1}H NMR spectra were recorded using 300 MHz Varian-Oxford Mercury.

Procedures

Potentiometric Measurements

The potentiometric measurements were obtained at 25 °C and ionic strength $\mu = 0.1$ by addition of appropriate amounts of 1 M sodium chloride solution. The pH-meter was calibrated before each titration using standard buffers. The ionization constants of the investigated Schiff base (HL^2) and the stability constants of its metal chelates with Fe(III), Co(II), Ni(II), Cu(II), Zn(II), and UO$_2$(II) ions were determined potentiometrically as described by Sarin and Munshi[18]. For this purpose, 3 solution mixtures of 50 mL were prepared. Thus,

A) 3 mL of standard HCl (around 0.10 M) + 5 mL 1 M NaCl + 25 mL ethanol, and the volume was completed up to 50 mL with distilled water.

B) 3 mL of 0.10 M HCl + 5 mL 1 M NaCl + 20 mL 0.001 M of ethanolic solution of the Schiff base (HL^2), and the volume was completed up to 50 mL with distilled water.

C) 3 mL of 0.10 M HCl + 5 mL 1 M NaCl + 20 mL 0.001 M of ethanolic solution of the Schiff base + 5 mL 0.001 M metal ion solution, and the volume being completed to 50 mL with distilled water.

The above 3 mixtures were titrated potentiometrically against standard sodium hydroxide solution (0.10 M). The molarities of HCl and NaOH were checked every day before the titrations. The appropriate volume of ethanol was added so as to keep a constant 50% ratio (v/v), ethanol/water, to ensure the complete solubility of the Schiff bases during the titration. The 3 curves obtained are referred to as: (A) acid titration curve, (B) ligand titration curve, and (C) complex titration curve.

Synthesis of Schiff base (L^1)[19]

A hot solution (60 °C) of o-phenylenediamine (1.08 g, 10 mmol) was mixed with a hot solution (60 °C) of 2-furancarboxaldehyde (1.92 g, 20 mmol) in 50 mL of ethanol. The resulting mixture was left under reflux for 2 h and the solid product formed was separated by filtration, purified by crystallization from ethanol, washed with diethyl ether, and then dried in a vacuum over anhydrous calcium chloride. The yellow product is produced in 80% yield.

Synthesis of Schiff base (HL^2) [20,21]

A hot solution (60 ℃) of 2-aminothiophenol (2.50 g, 10 mmol) in 25 mL of ethanol was mixed with a hot solution (60 ℃) of 2-thiophenecarboxaldehyde (2.24 g, 10 mmol) in the same solvent and the reaction mixture was left under reflux for 2 h. The solid product formed was separated by filtration, purified by crystallization from ethanol, washed with diethyl ether, and then dried in a vacuum over anhydrous calcium chloride. The yellow Schiff base product, HL^2, is produced in 80% yield.

Synthesis of metal complexes

The metal complexes of the Schiff bases, L^1 and HL^2, were prepared by the addition of a hot solution (60 ℃) of the appropriate metal chloride, nitrate, or acetate (1 mmol) in an ethanol-water mixture (1:1, 25 mL) to the hot solution (60 ℃) of the Schiff bases (0.264 g L^1 and 0.219 g HL^2, 2 mmol) in the same solvent (25 mL). The resulting mixture was stirred under reflux for 1 h whereupon the complexes precipitated. They were collected by filtration, washed with a 1:1 ethanol-water mixture and diethyl ether. The analytical data for C, H, N, and S were repeated twice.

Biological Activity

A 0.5 mL spore suspension (10^{-6}-10^{-7} spore/mL) of each of the investigated organisms was added to a sterile agar medium just before solidification, then poured into sterile petri dishes (9 cm in diameter) and left to solidify. Using a sterile cork borer (6 mm in diameter), 3 holes (wells) were made in each dish, and

then 0.1 mL of the tested compounds, dissolved in DMF (100 μg/mL), was poured into these holes. Finally, the dishes were incubated at 37 ℃ for 48 h. Then clear or inhibition zones were detected around each hole. DMF alone (0.1 mL) was used as a control under the same condition for each organism, and, by subtracting the diameter of inhibition zone resulting with DMF from that obtained in each case, both antibacterial activities were calculated as a mean of 3 replicates[22,23].

Results and Discussion

Schiff bases characterization

The Schiff bases, L^1 and HL^2, are subjected to elemental analyses. The results of elemental analyses (C, H, N, S) with molecular formulae and the melting points are presented in Tables 1 and 2. The results obtained are in good agreement with those calculated for the suggested formulae and the melting points are sharp, indicating the purity of the prepared Schiff bases. The structures of the Schiff bases under study are given below (Figure 1).

The structure of these Schiff bases is also confirmed by IR and ^{1}H NMR spectra, which will be discussed in a detailed manner, along with metal complexes, later. The electron impact mass spectra of L^1 and HL^2 were recorded and investigated at 70 eV of electron energy. The mass spectrum of L^1 shows a well-defined parent peak at m/z = 264 (M$^+$), with a relative intensity = 29%. The parent ion and the fragments obtained by cleavage in different positions in the L^1 molecule are shown in Scheme 1.
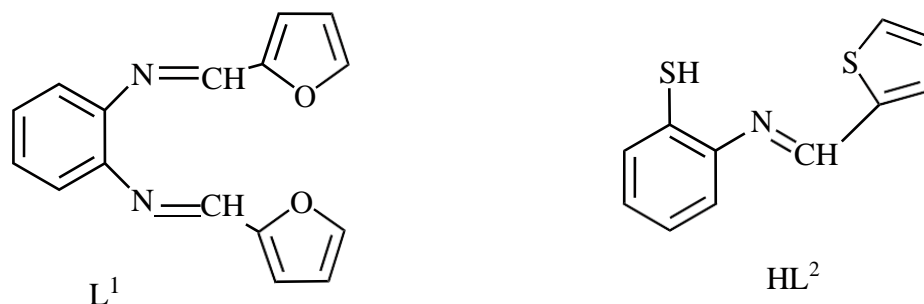
Figure 1. Structure of Schiff bases.

The mass spectrum of HL^2 shows a well-defined parent peak at m/z = 218, with a relative intensity = 15%. The fragment at m/z = 217 (R.I. = 100%, base peak) is attributed to the $C_{11}H_8NS$ ion as shown in the mass spectra of HL^2. The possible suggested molecular ion fragments, as the result of fragmentation of the parent molecule (HL^2), are given in Scheme 2.
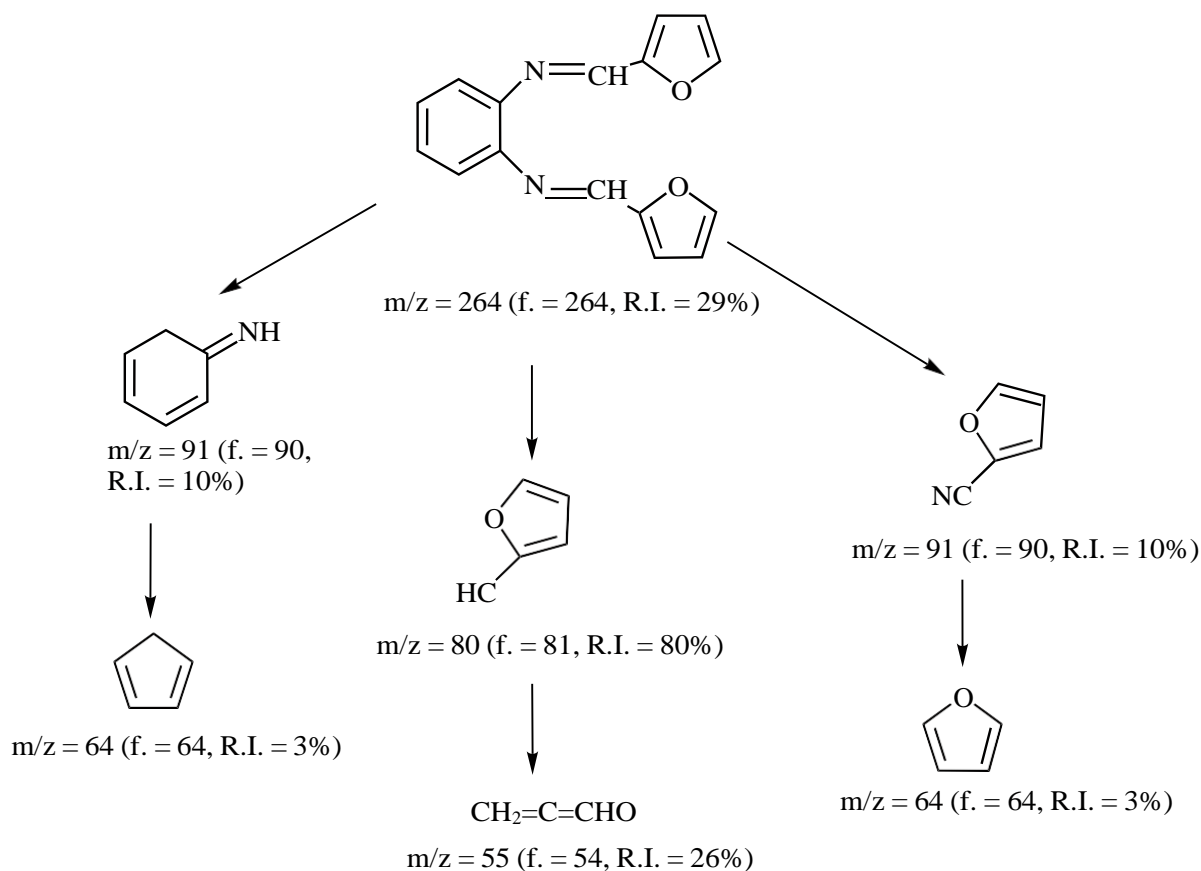
Table 1. Analytical and physical data of L^1 **and its complexes**.

Compound	Color % yield	M.p. °C)	% Found (calcd)				$\mu_{eff.}$ (B.M.)	$\Lambda_m\,\Omega^{-1}$ mol⁻¹cm²
			C	H	N	M		
L^1 $C_{16}H_{12}N_2O_2$	Yellow 88	78±2	72.52 (72.73)	7.98 (8.33)	10.43 (10.61)	——	—	—
[Fe(L^1)(H₂O)₂]Cl₃·3H₂O $C_{16}H_{22}Cl_3FeN_2O_6$	Brown 65	>300	37.4 (37.17)	3.89 (4.26)	5.78 (5.42)	11.06 (10.84)	5.53	315
[Co(L^1)]Cl₂·H₂O $C_{16}H_{14}Cl_2CoN_2O_3$	Brown 63	>300	46.2 (46.6)	3.18 (3.39)	6.38 (6.79)	14.07 (14.32)	5.24	175
[Ni(L^1)(H₂O)₂]Cl₂·4H₂O $C_{16}H_{24}Cl_2N_2NiO_8$	Brown 69	>300	38.3 (38.25)	4.49 (4.78)	5.27 (5.58)	11.83 (11.75)	3.8	187
[Cu(L^1)(H₂O)₂]Cl₂·2H₂O $C_{16}H_{20}Cl_2CuN_2O_6$	Brown 59	>300	40.54 (40.81)	4.19 (4.25)	6.02 (5.95)	13.33 (13.5)	2.07	222
[Zn(L^1)](AcO)₂·H₂O $C_{20}H_{20}N_2O_7Zn$	Brown 71	>300	41.65 (41.29)	4.56 (4.3)	6.17 (6.02)	13.63 (13.98)	Diam.	193
[UO₂(L^1)](NO₃)₂·3H₂O $C_{12}H_{18}N_4O_{11}U$	Brown 64	>300	26.64 (26.97)	2.74 (2.53)	8.19 (7.87)	——-	Diam.	210

The absorption spectra for 2.5 x 10^{-3}M solution of L^1 in absolute ethanol at λ ranging from 200 to 700 nm, against the same solvent as a blank, gives 3 sharp bands at 216 (ε = 1.96 x 10^3 L mol⁻¹ cm⁻¹), 244 (ε = 1.20 x 10^3 L mol⁻¹ cm⁻¹), and 308 (ε = 1.80 x 10^3 L mol⁻¹cm⁻¹), and a shoulder band at 370 nm (ε = 3.50 x 10^2 L mol⁻¹cm⁻¹), whereas the spectrum of HL^2(2.5 x 10^{-3}M solution in absolute ethanol at λ ranging from 200 to 700 nm, against the same solvent as a blank) shows 3 bands at 212 (ε = 1.58 x 10^3Lmol⁻¹cm⁻¹), 232 (ε = 6.00 x 10^2 L mol⁻¹cm⁻¹), 253 (ε = 5.00 x 10^2 L mol⁻¹cm⁻¹), and 326 nm (ε = 1.18x 10^3 L mol⁻¹cm⁻¹). These

bands can be attributed to π-π^* and n-π^* transitions within the Schiff bases.

m/z = 264 (f. = 264, R.I. = 29%)

m/z = 91 (f. = 90, R.I. = 10%)

m/z = 64 (f. = 64, R.I. = 3%)

m/z = 80 (f. = 81, R.I. = 80%)

$CH_2=C=CHO$

m/z = 55 (f. = 54, R.I. = 26%)

m/z = 91 (f. = 90, R.I. = 10%)

m/z = 64 (f. = 64, R.I. = 3%)

Scheme 1. Mass fragmentation pattern of L^1.

Table 2. Analytical and physical data of HL^2 and its complexes.

Compound	Color % yield	M.p. °C)	% Found (calcd)				$\mu_{eff.}$ (B.M.)	$\Lambda_m \, \Omega^{-1} \, mol^{-1} cm^2$
			C	H	N	M		
HL^2 $C_{11}H_9NS_2$	Yellow 82	180±2	59.97 (60.27)	4.32 (4.11)	6.19 (9.39)	28.87 (29.22)	——	——
$[Fe(L^2)_2]Cl\cdot2H_2O$ $C_{22}H_{20}ClFeN_2O_2S_4$	Brown 53	>300	46.63 (46.85)	3.82 (3.55)	5.12 (4.97)	22.5 (22.72)	10.05 (9.94)	5.92
$[Co(L^2)_2]$ $C_{22}H_{16}CoN_2S_4$	Black 50	>300	53.57 (53.33)	3.5 (3.23)	5.99 (5.66)	25.53 (25.86)	11.67 (11.92)	5.81
$[Ni(L^2)_2]\cdot2H_2O$ $C_{22}H_{20}N_2NiO_2S_4$	Brown 66	>300	50.07 (49.72)	3.55 (3.77)	5.55 (5.27)	23.89 (24.11)	11 (11.11)	3.97
$[Cu(L^2)_2]$ $C_{22}H_{16}CuN_2S_4$	Brown 61	>300	52.09 (52.85)	3.01 (3.2)	5.35 (5.61)	25.4 (25.63)	12.63 (12.71)	1.99
$[Zn(L^2)_2]$ $C_{22}H_{16}N_2S_4Zn$	Brown 60	>300	52.21 (52.69)	3.58 (3.19)	5.53 (5.59)	25.7 (25.55)	12.73 (12.97)	Diam.
$[UO_2(HL^2)_2](NO_3)_2$ $C_{22}H_{18}N_4O_8S_4U$	Black 65	>300	31.42 (31.73)	2.67 (2.16)	6.51 (6.73)	15.05 (15.38)	——-	Diam.

The ionization constant of the ionizable group in Schiff base HL^2 was determined by a method similar to that

–

described by Sarin and Munshi[18]. The average of protons associated with the ligand (n_A) at different pH values was calculated utilizing acid and ligand titration curves. The pK_a values can be calculated from

the curve obtained by plotting $n_{\overline{A}}$ versus pH. The formation curve was found between 0 and 1. This indicates that the ligand has one proton dissociable from the SH group. The pK_a value can also be calculated by plotting log $n_A/(1-n_A)$ versus pH, whereby a straight line is obtained intersecting the x-axis at the pK_a value. The average pK_a value, applying both methods, is found to be 9.06, and is attributed to the loss of a SH proton. The free energy change, ΔG^o, was also calculated and was 51.60 k.J.mol^{-1}. The positive value indicates the nonspontaneous character of the dissociation reaction.

The stability constants of the Ni(II), Co(II), Cu(II), UO$_2$(II), Fe(III), and Zn(II) complexes with HL^2 are determined potentiometriclly using the method described by Sarin[18] and Bjerrum[25]. The mean log β_1 and log β_2 values for complexes are listed in Table 3. The complex-forming abilities of the transition metal ions are frequently characterized by stability orders. The order of stability constants was found to be Co^{2+} < Ni^{2+} < Cu^{2+} > Zn^{2+}, in accordance with the Irving
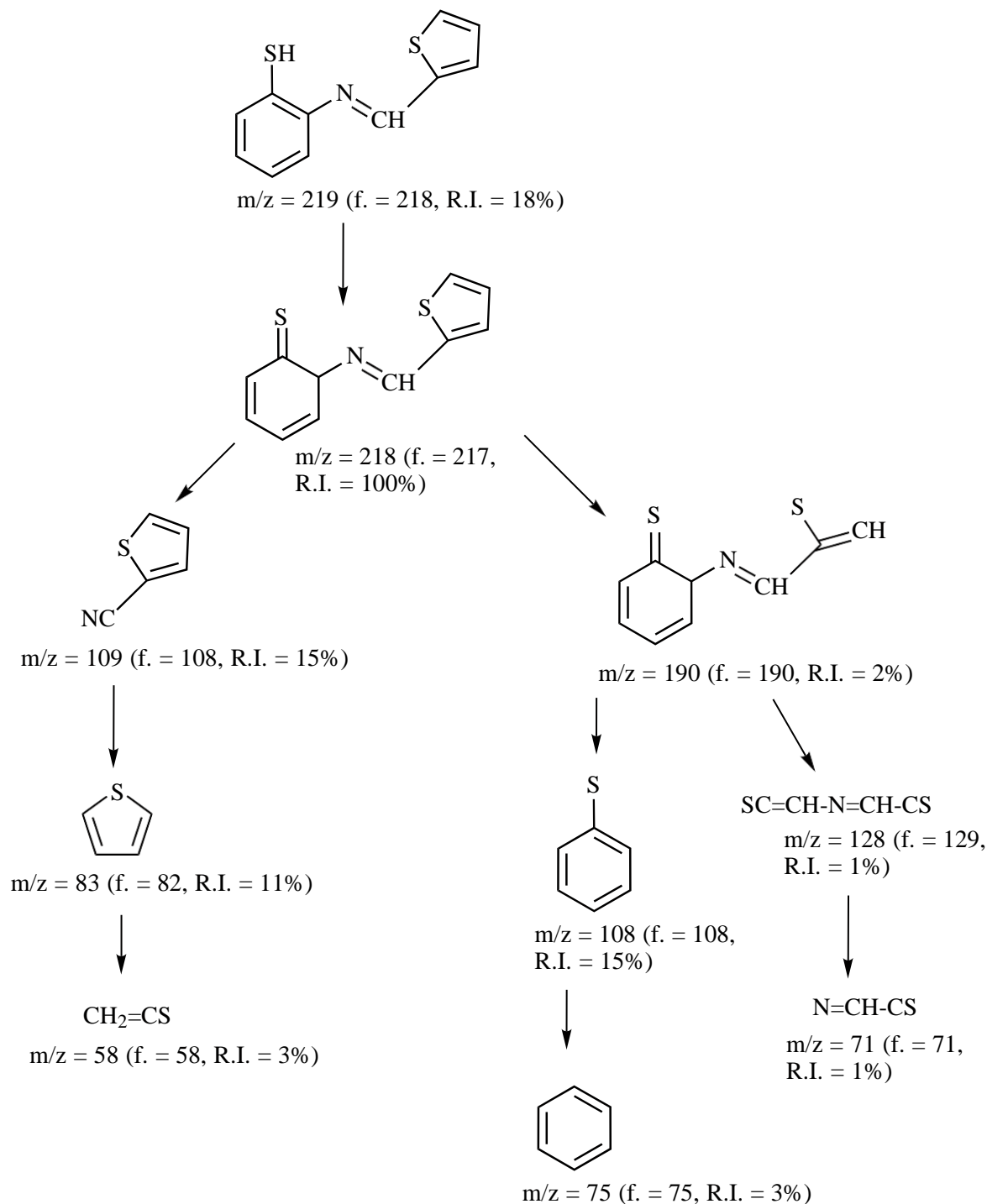
Williams order[26,27] for divalent metal ions of the 3d series. It is clear from Table 3 that the stability of Cu(II) complex is considerably more as compared to other metals of the 3d series. Under the influence of the ligand field, Cu(II) (3d^9) will receive some extra stabilization[28] due to tetragonal distortion of the octahedral symmetry in its complexes. The Cu(II) complex will be further stabilized due to the Jahn-Tellar effect[29].

The free energy of formation, ΔG^o, accompanying the complexation reaction was determined at 25 ° C. The results are given in Table 3. The negative values of ΔG^o show that the driving tendency of the complexation reaction is from left to right, and that the reaction proceeds spontaneously.

Composition and structures of Schiff bases complexes

Although L^1 [19] and HL^2 [20,21] ligands have been previously prepared, no studies concerning the Fe(III) and UO$_2$(II), Fe(III), Co(II), and UO$_2$(II) complexes for L^1 and HL^2 ligands, respectively, have been published. Hence, these complexes were prepared and thoroughly characterized. Additionally, the results reported herein are not in total agreement with the previously reported data. Moreover, the stability constants of the metal complexes of HL^2 ligand, as well as their thermal stability, have not been previously reported. A review of the literature revealed that the kinetic parameters calculated applying the Coats-Redfern method, together with the biological activities, have not been studied. Therefore, the main targets of this paper are to prepare the solid complexes of these ligands and to thoroughly characterize them using different physicochemical techniques, as well as studying their biological activities.

The isolated solid complexes of Fe(III), Co(II), Ni(II), Cu(II), Zn(II), and UO$_2$(II) ions with the Schiff bases' L^1 and HL^2 ligands were subjected to elemental analyses (C, H, N, S, and metal content), infrared spectral studies (IR), nuclear magnetic resonance (^{1}H NMR), magnetic studies, molar conductance, mass spectra, and thermal analysis (TGA) to identify their tentative formulae in an attempt to elucidate their molecular structures.

m/z = 219 (f. = 218, R.I. = 18%)

m/z = 218 (f. = 217, R.I. = 100%)

m/z = 109 (f. = 108, R.I. = 15%)

m/z = 190 (f. = 190, R.I. = 2%)

m/z = 83 (f. = 82, R.I. = 11%)

SC=CH-N=CH-CS

m/z = 128 (f. = 129, R.I. = 1%)

m/z = 108 (f. = 108, R.I. = 15%)

$CH_2=CS$

m/z = 58 (f. = 58, R.I. = 3%)

N=CH-CS

m/z = 71 (f. = 71, R.I. = 1%)

m/z = 75 (f. = 75, R.I. = 3%)

Scheme 2. Mass fragmentation pattern of HL[2].

Elemental analyses of the complexes

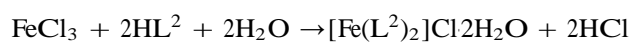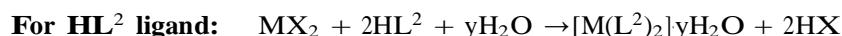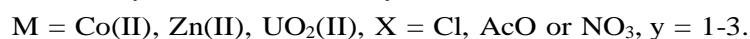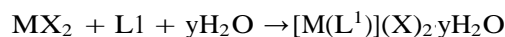The results of elemental analyses, as shown in Tables 1 and 2, are in good agreement with those required by the

proposed formulae. The formation of these complexes may proceed according to the following equations given below.

Table 3. Cumalative data of log β_1 and log β_2 values for complexes of HL^2 with Fe(III), UO_2(II), Co(II), Ni(II), Cu(II), and Zn(II).

Ion	$Log\beta_1$				$-\Delta G°$ (kJ.mol^{-1})	$Log\beta_2$				$-\Delta G°$ (kJ.mol^{-1})
	A	B	C	M		A	B	C	M	
Fe(III)	10.20	10.05	9.90	10.05	57.32	18.91	18.80	19.80	19.10	108.9
UO$_2$(II)	10.23	10.22	10.10	10.18	58.06	19.14	19.10	20.20	19.70	112.4
Co(II)	10.20	10.03	9.90	10.04	57.26	18.60	18.60	19.80	19.00	108.4
Ni(II)	10.32	10.62	9.900	10.28	58.63	19.34	19.30	19.80	19.60	111.8
Cu(II)	10.50	11.00	10.10	10.53	60.05	19.67	19.60	20.20	19.70	112.4
Zn(II)	10.40	10.68	9.99	10.35	59.03	19.36	19.30	19.90	19.40	110.6

Where (A) Interpolation at half values method. (B) Correction-term method. (C) Mid-point method. (M) Mean.

For L^1 ligand: $MCl_n + L^1 + 2H_2O + yH_2O \rightarrow [M(L^1)(H_2O)_2](Cl)_n yH_2O$

M = Fe(III), Ni(II), Cu(II); n = 2-3, y = 2-4.

$MX_2 + L1 + yH_2O \rightarrow [M(L^1)](X)_2 yH_2O$

M = Co(II), Zn(II), UO$_2$(II), X = Cl, AcO or NO$_3$, y = 1-3.

For HL^2 ligand: $MX_2 + 2HL^2 + yH_2O \rightarrow [M(L^2)_2]yH_2O + 2HX$

M = Co(II), Ni(II), Cu(II); X = Cl; y = 0-

2.M = Zn(II); X = AcO, y = 0.

$FeCl_3 + 2HL^2 + 2H_2O \rightarrow [Fe(L^2)_2]Cl\,2H_2O + 2HCl$

$UO_2(NO_3)_2 + 2HL^2 \rightarrow [UO_2(HL^2)_2](NO_3)_2$
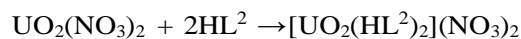
Molar conductivity measurements

By using the relation $\Lambda_m = K/C$, the molar conductance of the complexes (Λ_m) can be calculated, where C is the molar concentration of the metal complex solutions. The chelates were dissolved in DMF and the molar conductivities of 10^{-3} M of their solutions at 25 ± 2 °C were measured. Tables 1 and 2 show the molar conductance values of the complexes. It is concluded from the results that Fe(III) chelates of the L^1

and HL^2 ligands are found to have molar conductance values of 315 and 98 Ω^{-1} mol^{-1} cm^2, respectively, indicating the ionic nature of these complexes. Furthermore, it indicates the non-bonding of the chloride

anions to Fe(III). Consequently, the Fe(III) chelates are considered as 3:1 and 1:1 electrolytes with the L^1 and HL^2 ligands, respectively. On the other hand, the molar conductivity values of Co(II), Ni(II), Cu(II), and Zn(II) chelates with the L^1 ligand under investigation are in the range of 175 - 235 Ω^{-1} mol^{-1} cm^2, respectively. It is obvious from these data that these chelates are ionic in nature and they are of the type 2:1 electrolytes. The molar conductivity values of the metal chelates of HL^2 ligand (Λ_m = 8.97 -17.17 Ω^{-1} mol^{-1} cm^2) indicate that these complexes are non-electrolytes. UO$_2$(II) complexes of the L^1 and HL^2 ligands have molar conductivity values in the range of 193-217 Ω^{-1}mol^{-1}cm^2 (Tables 1 and 2). Based on these data, it is clear that these chelates are considered as 2:1 electrolytes, indicating the ionic nature of the bonding of the nitrate group to the cationic complex nucleus. According to previous data reported by Feng et al.[19], the Co(II), Ni(II), and Cu(II) complexes of L^1 ligand are non-electrolytes, but the data listed in Table 1 indicate the electrolytic nature of these complexes.

IR spectra and mode of bonding

The IR data of the spectra of Schiff base ligands (L^1 and HL^2) and their complexes are presented in Tables 4 and 5. The IR spectra of the complexes were compared with those of the free ligands in order to determine the coordination sites that may be involved in chelation. There were some guide peaks in the spectra of the ligands, which were helpful in achieving this goal. The position and/or the intensities of these peaks are expected to change upon chelation. New peaks are also guide peaks, as is water, in chelation. These guide peaks are shown in Tables 4 and 5. Upon comparison, it was determined that the v(C=N) stretching vibration is found in the free ligands at 1614 and 1659 cm^{-1} for the L^1 and HL^2 ligands, respectively. This band was shifted to higher or lower wavenumbers in the complexes, indicating the participation of the azomethine nitrogen in coordination (M—N) [30]. The SH stretching vibration, v(SH), is not useful, since it displayed very weak bands in both the free HL^2 ligand and complexes spectra. However, the participation of the SH group in chelation is ascertained from the shift of the v_{asym}(CS) and v_{sym}(CS) from 706 and 758 cm^{-1} to lower or higher wavenumbers in the spectra of the complexes[31]. Medium to sharp bands, due to v(C-O-C) stretching vibration of furan, appeared at 1229 cm^{-1} in the L^1 ligand[32]. This band disappeared or shifted to 1231-1274 cm^{-1} in L^1 metal complexes[33]. These shifts refer to the coordination through a furan

O atom. The sharp IR ligand bands at 824 cm^{-1}, v(C-S-C) of thiophene moiety, for the HL^2 ligand, shifted to 827-828 cm^{-1} for HL^2 metal complexes[34].

New bands are found in the spectra of the complexes in the regions 552-596 (furan O), which are assigned to v(M-O) stretching vibrations for L^1 metal complexes. The bands at 420-453 and 563-567 in L^1 and HL^2 metal complexes, respectively, have been assigned to v(M-N) mode. The v(M-S) bands appeared at 467-468 (thiophene) and 428-431 (thiophenol) for HL^2 metal complexes[35]. Therefore, from the IR spectra, it is concluded that the L^1 ligand behaves as a neutral tetradentate ligand coordinated to the metal ions via azomethine N and furan O; whereas HL^2 behaves as a uni-negtively terdentate ligand coordinated to the metal ions via deprotonated thiophenol S, azomethine N, and thiophene S; the exception is the UO_2(II) complex, where HL^2 behaves as a neutral ligand and is coordinated via its protonated SH group.

^{1}H NMR spectra

A review of the literature revealed that NMR spectroscopy has been proven to be useful in establishing the nature and structure of many Schiff bases, as well as their complexes in solutions. The NMR spectra of Schiff bases were recorded in d_6-dimethylsulfoxide (DMSO) solution, using tetramethylsilane (TMS) as internal standard. The NMR spectra of the Schiff bases, L^1 and HL^2, their diamagnetic Zn(II) complexes, and the chemical shifts of the different types of protons are listed in Table 6. The spectra of the complexes are examined in comparison with those of the parent Schiff bases. Upon examination it was found that the SH signal that appeared in the spectrum of the HL^2 ligand at 3.34 ppm completely[31] disappeared in the spectrum of its Zn(II) complex, indicating that the SH proton is removed by chelation with the Zn(II) ion. A new signal was observed at 1.82 ppm for Zn(II) complex with L^1, with an integration corresponding to 6 protons. The signals are assigned to 2 acetate molecules. Moreover, the signal that was observed at 3.34 ppm, with an integration corresponding to 2 protons in Zn(II) complexes with the L^1 ligand, is assigned to 1 water molecule.

Table 4. IR data (4000 – 400 cm^{-1}) of L^1 and its metal complexes.

Compound(C=N)	v (C-O-C)	v water)	v (OH) (Hydrated water)	δ (H$_2$O) (coordinated water)	v (M-O)	v (M-N)
L^1	1614sh	1229m	3349br	——-	——	——
[Fe(L^1)(H$_2$O)$_2$]Cl$_3$·3H$_2$O	1628sh	1237m	3320sh	928m, 884m	552s	432m
[Co(L^1)]Cl$_2$·H$_2$O	1626s	1232m	3401sh	931m, 884m	557s	452m
[Ni(L^1)(H$_2$O)$_2$]Cl$_2$·4H$_2$O	1611sh	1274m	3394br	928m, 883m	595m	420s
[Cu(L^1)(H$_2$O)$_2$]Cl$_2$·2H$_2$O	1617sh	1231sh	3381br	912m, 883m	657s	445m
[Zn(L^1)](AcO)$_2$·H$_2$O	1561sh	1240w	3115br	911s, 883s	596s	452s
[UO$_2$(L^1)](NO$_3$)$_2$·3H$_2$O	1628m	Disappear	3361br	943m, 885m	553m	453m

sh = sharp, m = medium, br = broad, s = small, w = weak

Table 5. IR data (4000-400 cm^{-1}) of HL^2 and its metal complexes.

Compound	v (SH)	v (C=N)	v (C-S-C)	v (CS) (asym)	v (CS) (sym)	v (M-S) (thiophenol)	v (M-S) (thiophene)	v (M-N)
HL^2	2371m	1659s	842sh	706sh	758sh	——-	——-	——-
[Fe(L^2)$_2$]Cl·2H$_2$O	2370s	1604ss	827sh	712sh	753sh	467m	428m	563m
[Co(L^2)$_2$]	2369s	1655w	828sh	710sh	761sh	469m	430m	568m
[Ni(L^2)$_2$]·2H$_2$O	2370s	1615w	828sh	710sh	761sh	468m	430m	568m
[Cu(L^2)$_2$]	2370s	1655w	828sh	709sh	761sh	468m	429m	565m
[Zn(L^2)$_2$]	2370w	1662s	827sh	709sh	753sh	468m	430m	567m
[UO$_2$(HL^2)$_2$](NO$_3$)$_2$	2370w	1651sh	828sh	709sh	753sh	469m	431m	567m

sh = sharp, m = medium, br =broad, s = small, w = weak

Magnetic susceptibility and electronic spectra measurements

From the diffuse reflectance spectra it is observed that the Fe(III) chelates exhibit a band at 20,491-22,026 cm^{-1}, which may be assigned to the $^6A_{1g} \rightarrow T_{2g}$ (G) transition in the octahedral geometry of the complexes[37]. The $^6A_{1g} \rightarrow {}^5T_1g$ transition appears to be split into 2 bands at 16,313 – 17,636 cm^{-1} and 12,626-13,020 cm^{-1}. The observed magnetic moments of Fe(III) complexes are 5.53-5.92.

B.M. Thus, the complexes formed have octahedral geometry involving d^{2}sp^3 hybridization in the Fe(III) ion[38]. The spectra also show a band at 23,641-25,510 cm^{-1}, which may be attributed to ligand to metal charge transfer. The Ni(II) complexes reported herein are high-spin with room temperature magnetic moment values of 3.80-4.02 B.M., which are in the normal range observed for octahedral Ni(II) complexes (μ_{eff} = 2.9-3.3 B.M)[39]. This indicates that the complexes of Ni(II) are 6-coordinate and probably octahedral[40]. Their electronic spectra, in addition to showing the π-π* and n-π* bands of free ligands, display 3 bands in the solid reflectance spectra at v_1: (12,690-13,987) cm^{-1}: $^3A_{2g} \rightarrow {}^3T_{2g}$, v_2: (15,649-16,155) cm^{-1}: $^3A_{2g} \rightarrow {}^3T_{1g}$(F), and v_3: (21,052-22,522) cm^{-1}: $^3A_{2g} \rightarrow {}^3T_{1g}$(P). Aditionally, the spectra show a band at 25,641-27,173 cm^{-1}, which may be attributed to ligand to metal charge transfer.

Table 6. Proton NMR spectral data of the Schiff bases and their metal chelates.

Compound	Chemical shift, (δ) ppm	Assignment
L^1	8.102	(s, 2H, azomethine H)
	5.83-7.84	(m, 10H, 4ArH and 6 furan H)
	3.7	(br, 2H, H_2O)
	2.5	(CH_3 of solvent)
$[Zn(L^1)](AcO)_2 \cdot 2H_2O$	8.01	(s, 2H, azomethine H)
	5.77-7.74	(m, 10H, 4ArH and 6 furan H)
	3.34	(br, 2H, H_2O)
	1.82	(s, 6H, CH_3COO)
	2.5	(CH_3 of solvent)
HL^2	3.34	(s, 1H, SH)
	7.22 – 8.10	(m, 8H, 4ArH, 1 azomethine, 3 thiophene H)
	2.5	($CH_3$of solvent)
$[Zn(L^2)_2]$	———	———
	7.22 – 8.10	(m, 16H, 8ArH, 2 azomethine, 6 thiophene H)
	2.5	($CH_3$of solvent)

The reflectance spectrum of Co(II) complex with L^1 gives a high-energy transition, 4A2 $\rightarrow^4T_1$(P), for tetrahedral transition at 14,900 cm^{-1}. Moreover, a transition, $^4A_2 \rightarrow^4T_1$ (F), as well as one quite low energy $\rightarrow$transition, $^4A_2 \rightarrow^4T_2$, were observed at 16,649 and 19,600 cm^{-1}, respectively. The magnetic susceptibility measurement (μ_{eff} = 5.24 B.M.) is indicative of tetrahedral geometry[39,41]. This result is not in agreement with previously reported data[19], which suggest octahedral geometry.

The electronic spectra of the Co(II) complex with HL^2 gives 3 bands at 13,157, 16,474, and 22,123 cm^{-1} wavenumber regions. The region at 25,445-27,027 cm^{-1} refers to the charge transfer band. The bands observed are assigned to the transitions, $^4T_{1g}$(F) $\rightarrow ^4T_{2g}$(F) (v_1), $^4T_{1g}$ (F) $\rightarrow ^4A_{2g}$(F) (v_2), and 4T_{1g} (F) $\rightarrow ^4T_{2g}$(P) (v_3), respectively, suggesting that there is an octahedral geometry around the Co(II) ion[30,43−45]. The magnetic susceptibility measurements lie in the 5.57-5.81 B.M. range (normal range for octahedral Co(II) complexes is 4.3-5.2 B.M.), which is indicative of octahedral geometry[46].

The reflectance spectra of Cu(II) chelates consist of a broad, low intensity shoulder band centered at 15,873-16,420 and 17,543-22,026 cm^{-1}. The ^2E_g and $^2T_{2g}$ states of the octahedral Cu(II) ion (d^9) split under the influence of the tetragonal distortion, and the distortion can be such as to cause the 3 transitions, $^2B_{1g} \rightarrow^2B_{2g}$, $^2B_{1g} \rightarrow^2E_g$, and $^2B_{1g} \rightarrow^2A_{1g}$, to remain unresolved in the spectra[47]. It is concluded that all 3 transitions lie within the single broad envelope centered at the same range previously mentioned. This assignment is in agreement with the general observation that Cu(II) d-d transitions are normally close in energy[48]. The magnetic moment of 1.93-2.07 B.M. falls within the range normally observed for octahedral Cu(II) complexes[49]. A moderately intense peak observed in the range of 21,459-26,455 cm^{-1} is due to ligand-metal charge transfer transition[50].

The complexes of Zn(II) and UO_2(II) are diamagnetic. In analogy with those described for Zn(II) complexes containing N-O donor Schiff bases[51−53] and according to the empirical formulae of these com- plexes, we proposed an octahedral geometry for the Zn(II) complexes of HL^2, while the Zn(II) complex of L^1 has a tetrahedral geometry. The UO_2(II) complexes are octahedral.

Thermal analyses (TGA and DrTG)

Thermogravimetric analyses (TGA and DrTA) of the Schiff base ligands, L^1 and HL^2, and their chelates are used to: (i) get information about the thermal stability of these new complexes, (ii) decide whether the water molecules (if present) are inside or outside the inner coordination sphere of the central metal ion, and (iii) suggest a general scheme for thermal decomposition of these chelates. In the present investigation, heating rates were suitably controlled at $10\,°C\,min^{-1}$ under nitrogen atmosphere, and the weight loss was measured

from the ambient temperature up to $\cong 1000\,°C$. The data are provided in Tables 7 and 8. The weight loss for each chelate was calculated within the corresponding temperature ranges. The TGA curve of Schiff base L^1 exhibits a first estimated mass loss of 49.93% (calcd: 50.76%) at 30-400 °C, which may be attributed to the liberation of $C_8H_6O_2$ as gases. In the 3rd and 4th stages within the temperature range 400-900 °C, L^1 loses the remaining part with an estimated mass loss of 50.07% (calcd: 49.24%) with a complete decomposition as CO, CO_2, NO, NO_2, etc. gases. The TGA curve of Schiff base HL^2 showed that this ligand decomposed in one step, from 180 to 400 °C. This step corresponds to the complete decomposition of HL^2 as deduced from mass loss calculation (found mass loss = 100.0%, calcd. mass loss = 100.0%). Tables 7 and 8 show the TGA and DrTGA results of thermal decomposition of the Schiff base chelates. The thermogram of the Fe(III)-HL^2 chelate shows 3 decomposition steps within the temperature range 25-700 °C, whereas the Fe(III)-L^1 chelate shows 5 decomposition steps within the temperature range 30-1000 °C. The first 2 steps of decomposition within the temperature range 25-500 °C correspond to the loss of water molecules of hydration and HCl, H_2, and O_2 gases, with a mass loss of 28.13% (calcd: 27.59%) for the Fe(III)-L^1 chelate, while the first step in the Fe(III)-L^2 chelate occurs within the temperature range 50-320 °C, which corresponds to the removal of HCl and $C_{16}H_{13}NS_3$, with a mass loss of 61.89% (calcd: 62.38%). The subsequent steps (280-1000 °C) correspond to the removal of the organic part of the ligands, leaving metal oxide as a residue. The overall weight loss amounts to 86.01% (calcd: 84.52%) and 85.72% (calcd: 85.81%) for the Fe(III) chelates with L^1 and HL^2 ligands, respectively.

The TGA curves of the Ni(II)-chelates, show 3 to 5 stages of decomposition within the temperature range of 30-900 °C. The first stage, at 30-120 °C, corresponds to the loss of water molecules of hydration, while the subsequent (2nd, 3rd, 4th, and 5th) stages involve the loss of HCl, H_2O, $\frac{1}{2}$ O_2, and ligand molecules. The overall weight loss amounts to 85.18% (calcd: 85.06%) and 85.85% (calcd: 85.88%) for the Ni(II) chelate with L^1 and HL^2 ligands, respectively. On the other hand, $[Cu(L^1)(H_2O)_2]Cl_2·2H_2O$ and $[Cu(L^2)_2]$ chelates exhibit 1 to 4 decomposition steps. For the Cu(II)-L^1 chelate, the first step is in the temperature range 30-120 °C (mass loss = 7.96%; calcd for $2H_2O$: 7.65%), which may account for the loss of water molecules of hydration. As shown in Tables 7 and 8, the mass losses of the remaining decomposition steps amount to 22.85% (calcd: 22.74%) and correspond to the removal of HCl, H_2O, $\frac{1}{2}$ O_2, L^1 molecules, leaving CuO as a residue. $[Cu(L^2)_2]$ complex undergoes 1 step of decomposition within the temperature range 100-500 °C, with an estimated mass loss of 83.09% (calcd: 83.01%). This mass loss corresponds to the pyrolysis of the 2 ligand molecules leaving $\frac{1}{2}$ Cu_2S as a residue.

Table 7. Thermoanalytical results (TG, DrTG) of L^1 and its metal complexes.

Complex	TG range (°C)	DrTG$_{max}$ (°C)	n*	Mass loss Estim (Calcd.) %	Total mass loss Estim (Calcd.) %	Assignment	Metallic residue
L^1	30-400	70, 267	2	49.93 (50.76)		- Loss of $C_8H_6O_2$.	——
	400-900	570, 758	2	50.07 (49.24)	100.0 (100.0)	- Loss of $C_8H_6N_2$.	
	30-130	63	1	10.83 (10.46)		- Loss of $3H_2O$.	
(1)	130-500	182, 320	2	28.13 (27.59)		- Loss of 3HCl, $\frac{1}{2}$ H_2 and O_2.	$\frac{1}{2}$ Fe_2O_3
	500-1000	620, 880	2	47.05 (46.47)	86.01 (84.52)	- Loss of $C_{16}H_{12}N_2O_{0.5}$.	
	30-100	79	1	14.89 (14.34)		- Loss of $4H_2O$.	
(2)	100-280	170, 260	2	20.99 (21.32)		- Loss of 2HCl, $\frac{1}{2}$ O_2 and H_2O.	NiO
	280-700	410, 660	2	49.30 (49.40)	85.18 (85.06)	- Loss of $C_{16}H_{12}N_2O$.	
	30-120	88	1	7.96 (7.65)		- Loss of $2H_2O$.	
(3)	120-470	195, 280	2	22.83 (22.74)		- Loss of 2HCl, $\frac{1}{2}$ O_2 and H_2O.	CuO
	470-850	740	1	53.11 (52.71)	83.90 (83.10)	- Loss of $C_{16}H_{12}N_2O$.	
	25-120	40, 90	2	7.58 (7.20)		- Loss of $3H_2O$.	
(4)	120-280	150	1	17.42 (17.88)		- Loss of $2NO_2$ and O_2.	UO_2
	280-650	320, 510	2	37.08 (37.37)	62.05 (62.45)	- Loss of $C_{16}H_{12}N_2O_2$.	

n* = number of decomposition steps (**1**) $[Fe(L^1)(H_2O)_2]Cl_3 \cdot 3H_2O$, (**2**) $[Ni(L^1)(H_2O)_2]Cl_2 \cdot 4H_2O$, (**3**) $[Cu(L^1)(H_2O)_2]Cl_2 \cdot 2H_2O$, (**4**) $UO_2(L^1)](NO_3)_2 \cdot 3H_2O$

Table 8. Thermoanalytical results (TG, DrTG) of metal complexes HL^2.

Complex	TG range (°C)	DrTG$_{max}$ (°C)	n*	Mass loss Estim (Calcd.) %	Total mass loss Estim (Calcd.) %	Assignment	Metallic residue
HL^2	180-400	300	1		100.0 (100.0)	- Loss of $C_{11}H_9NS_2$.	——
(5)	50-320	280	1	61.89 (62.38)		- Loss of HCl and $C_{16}H_{13}NS_3$.	
	320-700	550, 640	2	86.01 (84.52)	85.72 (85.81)	- Loss of $C_6H_6NO_{0.5}S$.	$\frac{1}{2}$ Fe_2O_3
(6)	30-100	60	1	3.75 (3.39)		- Loss of H_2O.	
	100-700	275, 550	2	82.10 (82.49	85.85 (85.88)	- Loss of $C_{22}H_{18}N_2S_4$.	NiO
(7)	100-500	265	1		83.90 (83.10)	- Loss of $C_{22}H_{16}N_2S_{3.5}$.	$\frac{1}{2}$ Cu_2S
(8)	50-150	137	1	15.07 (14.90)		- Loss of $2NO_2$ and O_2.	
	150-650	240, 430	2	53.06 (52.64)	68.13 (67.54)	- Loss of $C_{22}H_{18}N_2S_4$.	UO_2

n* = number of decomposition steps (**5**) $[Fe(L^2)_2]Cl \cdot 2H_2O$, (**6**) $[Ni(L^2)_2] \cdot H_2O$, (**7**) $[Cu(L^2)_2]$, (**8**) $[UO_2(HL^2)_2](NO_3)_2$.

The TGA curves of the $UO_2(II)$ chelates represent 3 to 5 decomposition steps, as shown in Tables 7 and 8. For the $UO_2(II)$-L^1 chelate, the first step of decomposition within the temperature range 25-120 ˚C corresponds to the loss of hydrated water molecules, with a mass loss of 7.58% (calcd for $3H_2O$: 7.20%), while the first step of decomposition for the $UO_2(II)$-L^2 complex corresponds to the loss of 2 nitrate moieties into $2NO_2$ and O_2 gases, within the temperature range 50-150 ˚C (mass loss: 15.07%; calcd: 14.90%). The remaining steps of decomposition within the temperature range 120-800 ˚C correspond to the removal of these ligands as gases. The overall weight losses amount to 62.05% (calcd: 62.45%) and 68.13% (calcd: 67.54%) for $UO_2(II)$-L^1 and $UO_2(II)$-L^2 chelates, respectively.

Calculation of activation thermodynamic parameters

The thermodynamic activation parameters of decomposition processes of dehydrated complexes, namely activation energy (E^*), enthalpy (ΔH^*), entropy (ΔS^*), and Gibbs free energy change of the decomposition (ΔG^*), were evaluated graphically by employing the Coats-Redfern relation[54]:

$$\log \frac{\log\{W_f/W_f-W)\}}{T^2} = \log \frac{AR}{\theta E^*}\left[1 - \frac{2RT}{E^*}\right] - \frac{E^*}{2.303RT} \tag{1}$$

where W_f is the mass loss at the completion of the reaction, W is the mass loss up to temperature T, R is the gas constant, E^* is the activation energy in $kJ.mol^{-1}$, θ is the heating rate, and $(1-(2RT/E^*)) \cong 1$. A plot of the left-hand side of equation (1) against $1/T$ gave a slope from which E^* was calculated and A (Arrhenius factor) was determined from the intercept. The entropy of activation (ΔS^*), enthalpy of activation (ΔH^*), and the free energy change of activation (ΔG^*) were calculated using the following equations:

$$\Delta S^* = 2.303[log(Ah/kT)]R \tag{2}$$

$$\Delta H^* = E^* - RT \tag{3}$$

$$\Delta G^* = \Delta H^* - T\Delta S^* \tag{4}$$

The data are summarized in Tables 9 and 10. The activation energies of decomposition were in the range 55.42-350.6 $kJ\ mol^{-1}$. The high values of the activation energies reflect the thermal stability of the complexes. The entropy of activation had negative values in all the complexes, which indicates that the decomposition reactions proceed with a lower rate than the normal ones.

Structural interpretation

The structures of the complexes of Schiff bases L^1 and HL^2, with Fe(III), Co(II), Ni(II), Cu(II), Zn(II), and $UO_2(II)$ ions were confirmed by elemental analyses, IR, NMR, molar conductance, magnetic, solid reflectance, UV-Vis, mass, and thermal analysis data. Therefore, from the IR spectra, it is concluded that L^1 behaves as a neutral tetradentate ligand, coordinated to the metal ions via azomethine N and furan O. HL^2 behaves as a uni-negatively terdentate ligand, coordinated to the metal ions via deprotonated thiophenol S, azomethine N, and thiophene S, with the exception of the $UO_2(II)$ complex, where it behaves as a neutral ligand and is coordinated via its protonated SH group. From the molar conductance data, it was found that the Fe(III) chelates are considered as 3:1 and 1:1 electrolytes. On the other hand, the molar conductivity

values of Co(II), Ni(II), Cu(II), and Zn(II) chelates with the L^1 ligand under investigation are ionic in nature and they are of the type 2:1 electrolytes, while their complexes with the HL^2 ligand are non-electrolytes. $UO_2(II)$ complexes of L^1 and HL^2 ligands are considered as 2:1 electrolytes. The ^1H NMR spectra of the free ligands and their diamagnetic Zn(II) complexes show that the SH signal appeared in the spectrum of the HL^2 ligand at 3.34 ppm and completely disappeared in the spectrum of its Zn(II) complex, indicating that the SH proton is removed by chelation with the Zn(II) ion. On the basis of the above observations and from the magnetic and solid reflectance measurements, octahedral and tetrahedral geometries are suggested for the investigated complexes.

Table 9. Thermodynamic data of the thermal decomposition of metal complexes of L^1.

Complex	Decomp. Temp. (C)	E* kJmol^{-1}	A s^{-1}	Δ S* KJmol^{-1}	Δ H* kJmol^{-1}	Δ G* kJmol^{-1}
$[Fe(L^1)(H_2O)_2]Cl_3\cdot 3H_2O$	30-130	35.73	1.23×10^5	-108	73.48	72.65
	130-220	49.14	4.05×10^7	-136	61.49	96.2
	220-430	93.34	4.51×10^{10}	-224	98.39	48.68
	570-700	119.54	6.23×10^9	-104.6	101.6	66.5
	820-960	135	5.01×10^{10}	-202.6	96.43	88.08
$[Ni(L^1)(H_2O)_2]Cl_2\cdot 4H_2O$	30-100	55.43	2.13×10^6	-116	42.83	41.51
	130-210	73.81	6.03×10^7	-108	73.61	78.97
	230-280	86.35	3.68×10^{12}	-56.06	28.69	91.36
	360-430	215.2	9.33×10^{10}	-63.96	195	206
	460-660	343	6.18×10^{14}	-165.1	232	320
$[Cu(L^1)(H_2O)_2]Cl_2\cdot 2H_2O$	30-120	80.8	4.21×10^{10}	-35.69	73.12	87.32
	120-210	145.7	8.69×10^{14}	-109.8	194.5	156
	210-450	223.7	5.89×10^{16}	-184.9	262.3	201.3
	500-800	267.2	4.01×10^{10}	-65.78	218.4	284.2
$[UO_2(L^1)](NO_3)_2\cdot 3H_2O$	25-60	95.76	2.29×10^9	-59.21	67.73	85.66
	60-110	118.5	7.04×10^{16}	-45.34	135.4	166.8
	110-200	222.3	6.86×10^{12}	-50.52	227.6	205.9
	280-360	318.5	6.58×10^{15}	-126.9	341.9	305.1
	440-520	125.3	5.08×10^{11}	-96.53	102.9	165.2

**Table 10.** Thermodynamic data of the thermal decomposition of metal complexes of HL^2.

Complex	Decomp. Temp. (°C)	E* kJmol^{-1}	A s^{-1}	Δ S* kJmol^{-1}	Δ H* kJmol^{-1}	Δ G* kJmol^{-1}
$[Fe(L^2)_2]Cl\cdot 2H_2O$	50-300	47.35	4.09×10^8	-108	48.73	72.2
	470-650	74.59	5.95×10^{10}	-156.6	49.69	86.7
	700-800	99.33	3.66×10^{12}	-204.3	88.93	58.89
$[Ni(L^2)_2]H_2O$	30-100	45.45	3.29×10^7	-126.8	74.83	49.98
	180-300	73.61	9.83×10^9	-188.7	165.87	107.4
	500-650	205	7.99×10^{12}	-205.4	240.6	199.9
$[Cu(L^2)_2]$	150-300	195.7	6.08×10^{18}	-109.8	249.2	170.6
$[UO_2(HL^2)_2](NO_3)_2$	50-150	79.97	4.27×10^{12}	-45.34	136.6	126.4
	170-300	148.5	7.67×10^9	-73.99	217.8	215.7
	350-500	232.8	6.55×10^{16}	-116.1	281.6	271.9

As a general conclusion, the investigated Schiff bases behave as a tetradentate (L^1) or tridentate(HL^2), and their metal complex structures can be given as shown below (Figures 2 and 3).
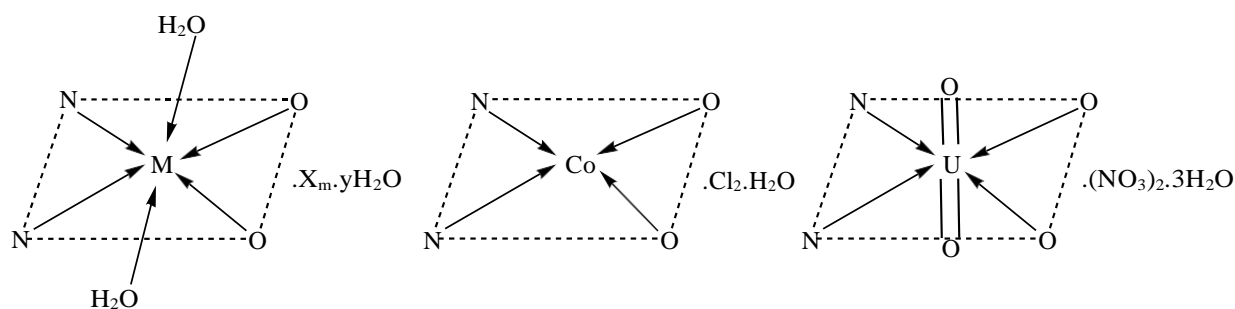
M = Fe(III), X = Cl, m = 3, y = 3.
  Ni(II), X = Cl, m = 2, y = 4.
  Cu(II), X = Cl, m = 2, y = 2.
  Zn(II), X = AcO, m = 2, y = 1.

Figure 2. Structural formulae of L^1metal complexes.
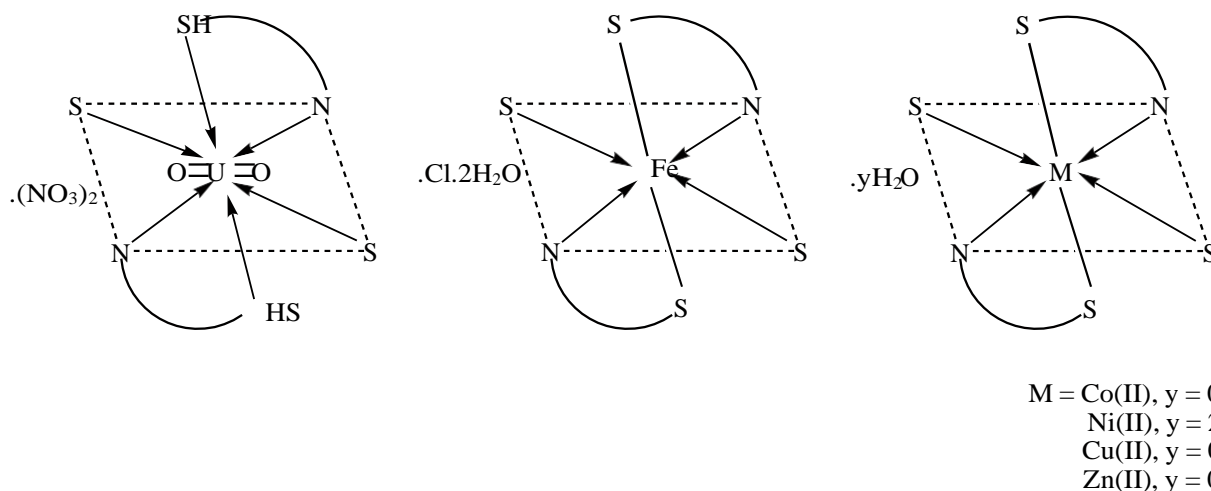
M = Co(II), y = 0.
  Ni(II), y = 2.
  Cu(II), y = 0.
  Zn(II), y = 0.

Figure 3. Structural formulae of HL^2metal complexes.

Biological Activity

In testing the antibacterial activity of these compounds we used more than one test organism to increase the chance of detecting the antibiotic potential of the tested materials. The sensitivity of a microorganism to antibiotics and other antimicrobial agents was determined by the assay plates, which were incubated at 28 °C for 2 days (for yeasts) and at 37 °C for 1 day (for bacteria). All of the tested compounds showed a remarkable biological activity against different types of Gram-positive and Gram-negative bacteria. The data are listed in Tables 11 and 12. Upon comparison of the biological activity of the Schiff bases and their metal complexes with the standard (Traivid and Tavinic), it is seen that the biological activity of the

Schiff bases increases in the order $HL^2 > L^1$. The biological activity of L^1 and HL^2 are less than that of Tavinic, but higher than that of Traivid. For Schiff base (L^1) complexes, the biological activity of Fe(III), Co(II), Cu(II), and $UO_2(II)$ complexes is higher than that of the ligand and Traivid, while their activity is comparable with that of standard Tavinic. For Ni(II) and Zn(II) complexes, their biological activity is nearly

the same as that of L^1. The biological activity of the complexes follow the order Fe(III) = Co(II) =

$Cu(II) = UO_2(II) > Zn (II) > Ni(II)$. On the other hand, for Schiff base (HL^2) complexes, the biological activity of Fe(III), Ni(II), Zn(II), and $UO_2(II)$ complexes is nearly the same as the ligand, less than standard Tavinic, and higher than that of standard Traivid. The biological activity of Co(II) and Cu(II) complexes is nearly identical as that of standard Tavinic, higher than that of the HL^2 ligand, and higher than that of standard Traivid. The biological activity of the complexes follow the order, $Co(II) = Cu(II) > Fe(III) = UO_2(II) > Zn (II) = Ni(II)$.

Furthermore, the data in Tables 11 and 12 show that *E. coli* was inhibited by Ni(II), Zn(II), and $UO_2(II)$ complexes, and Fe(III) and Ni(II) complexes of L^1 and HL^2 ligands, respectively. The importance of this lies in the fact that these complexes could reasonably be used for the treatment of some common diseases caused by *E. coli*, e.g., septicemia, gastroenteritis, urinary tract infections, and hospital-acquired infections[55,56].

Table 11. Biological activity of L^1 and its metal complexes.

Sample	Staphylococcus pyogenes			Pseudomonas aeruginosa			Fungus (Candida) (Candida)			Escherichia coli		
C, mg/L	5	2.5	1	5	2.5	1	5	2.5	1	5	2.5	1
L^1	++	++	+	++	+	+	+	-	-	++	+	-
$[Fe(L^1)(H_2O)_2]Cl_3 \cdot 3H_2O$	+++	++	+	++	++	+	+	+	-	++	++	+
$[Co(L^1)]Cl_2 \cdot H_2O$	+++	++	+	++	++	+	+	-	-	++	+	+
$[Ni(L^1)(H_2O)_2]Cl_2 \cdot 4H_2O$	++	+	-	++	+	+	+	-	-	+++	++	+
$[Cu(L^1)(H_2O)_2]Cl_2 \cdot 2H_2O$	+++	++	++	+++	++	+	+	-	-	++	++	+
$[Zn(L^1)](AcO)_2 \cdot H_2O$	++	+	+	++	+	-	+	-	-	+++	++	+
$[UO_2(L^1)](NO_3)_2 \cdot 3H_2O$	+++	++	+	++	++	+	+	+	-	+++	++	+
Traivid	++	+	-	++	+	-	-	-	-	++	+	-
Tavinic	+++	++	+	+++	++	+	-	-	-	+++	++	+

The test was performed using the diffusion agar technique. Inhibition values = 0.1-0.5 cm beyond control = + Inhibition values = 0.6-1.0 cm beyond control = ++ Inhibition values = 1.1-1.5 cm beyond control = +++

Table 12. Biological activity of HL^2 and its metal complexes.

Sample	Staphylococcus pyogenes			Pseudomonas aeruginosa			Fungus (Candida) (Candida)			Escherichia coli		
C, mg/L	5	2.5	1	5	2.5	1	5	2.5	1	5	2.5	1
HL^2	++	++	+	++	+	-	+	-	-	++	+	+
$[Fe(L^2)_2]Cl \cdot 2H_2O$	++	++	+	++	++	+	+	+	-	+++	++	+
$[Co(L^2)_2]$	+++	++	+	++	+	-	+	-	-	++	++	+
$[Ni(L^2)_2] \cdot 2H_2O$	++	+	+	+++	++	+	+	-	-	+++	++	+
$[Cu(L^2)_2]$	+++	++	+	++	+	+	+	-	-	++	++	+
$[Zn(L^2)_2]$	++	+	+	++	+	+	+	+	-	++	++	+
$[UO_2(HL^2)_2](NO_3)_2$	++	++	+	+++	++	+	+	+	-	++	+	+
Traivid	++	+	-	++	+	-	-	-	-	++	+	-
Tavinic	+++	++	+	+++	++	+	-	-	-	+++	++	+

The test was performed using the diffusion agar technique. Inhibition values = 0.1-0.5 cm beyond control = + Inhibition values = 0.6-1.0 cm beyond control = ++ Inhibition values = 1.1-1.5 cm beyond control = +++

However, Fe(III), Cu(II), and $UO_2(II)$, and Co(II), Ni(II), Cu(II), and $UO_2(II)$ complexes of L^1 and HL^2 ligands, respectively, were specialized in inhibiting Gram-positive bacterial strains (*Staphylococcus*

pyogenes and *Pseudomonas aeruginosa*). The importance of this unique property of the investigated Schiff base complexes is that they could be administered safely for the treatment of infections caused by any of these particular strains. In addition, all metal complexes of L^1 and Fe(III), Zn(II), and UO_2(II) complexes of HL^2 inhibit fungi at high concentration (5 mg/L), more so than the parent ligands and standards. Therefore, it is claimed here that such compounds might have a possible antitumor effect since Gram-negative bacteria are considered a quantitative microbiological method for testing beneficial and important drugs, in both clinical and experimental tumor chemotherapy[57,58].

References

1. R.D. Jones, D.A. Summerville and F. Basolo, **Chem. Rev. 79**, 139 (1979).

2. G.H. Olie and S. Olive, "**The Chemistry of the Catalyzes Hydrogenation of Carbon Monoxide**", p.152, Springer, Berlin, 1984.

3. H. Dugas and C. Penney, "**Bioorganic Chemistry**", p. 435, Springer, New York, 1981.

4. J.D. Margerum and L.J. Mller, "**Photochromism**", p. 569, Wiley Interscience, New York, 1971.

5. W.J. Sawodny and M. Riederer, **Angew. Chem**. **Int. Edn. Engl. 16**, 859 (1977).

6. A.S. Salameh and H.A. Tayim, **Polyhedron**, **2,** 829-34 (1983).

7. H.A. Tayim and A.S. Salameh, **Polyhedron, 2,** 1091-4 (1983).

8. B.T. Thaker, **Proc. Natl. Acad. Sci. India, Sect. A, 58,** 443-7 (1988).

9. S.D. Kolwalkar and B.H. Mehta, **Asian J. Chem. 8,** 406-410 (1996).

10. M.A. Khalifa and A.M. Hassaan, **J. Chem. Soc. Pak. 18,** 115-118 (1996).

11. Y.M. Issa, M.M. Omar, H.M. Abdel-Fattah and A.A. Soliman, **J. Indian Chem. Soc. 73**, (1996).

12. J.J. Murthy and B.H. Mehta, **Orient. J. Chem. 14,** 129-131 (1998).

13. S. Zhou, S. Liu and G. Zhou, **Huaxue Shiji, 23,** 26-27 (2001).

14. N. Raman, A. Kulandaisamy and K. Jeyasubramanian, **Synth. React. Inorg. Met.-Org. Chem. 31,** 1249-1270 (2001).

15. S. Zhou, F. Xie and S. Ni, **Huaxue Shiji, 23,** 261-262 (2001).

16. A.I. Vogel, "**Practical Organic Chemistry Including Quantitative Organic Analysis**", 3rd Ed., p. 854,Longmans; London, 1956.

17. A.I. Vogel, "**Quantitative Inorganic Analysis Including Elemental Instrumental Analysis**", 2nd Ed.,Longmans; London, 1962.

18. R. Sarin and K.N. Mushi, **J. Inorg. Nucl. Chem. 34**, 581 (1972).

19. D. Feng and B. Wang, **Transition Met. Chem. 18,** 101-3 (1993). M. Kumar, **Asian J. Chem. 6,** 576-80(1994).

20. F. Capitan, P. Espinosa, F. Molina and L.F. Capitan-Vallvey, **Rev. Roum. Chim. 32,** 151-4 (1987).

21. H.A. Tayim and A.S.S. Salameh, **Polyhedron, 2,** 10, 1091-4 (1983).

22. M.E. Ibrahim, A.A.H. Ali and F.M.M. Maher, **J. Chem. Techn. Biotechnol. 55**, 217 (1992).

23. N. Sari, S. Arslan, E. Logoglu and I. Sakiyan, **J. of Sci. 16**, 283 (2003).

24. J. Bjerrum, "**Metal Amine Formation in Aqueous Solution**", Haase, Copenhagen, 1941.

25. H. Irving and R.J.P. Williams, **Nature, 162**, 746 (1948).

26. H. Irving and R.J.P. Williams, **J. Chem. Soc.** 3192 (1953).

27. R.D. Jones, D.A. Summerville and F. Basolo, **Chem. Rev. 79**, 139 (1979).

28. L.E. Orgel, "**An Introduction to Transition Metal Chemistry Ligand Field Theory**", p.55, Methuen,1966.

29. G.G. Mohamed, Zeinb H.Abd El.Wahwb, **J. Thermal Anal. 73**, 347-359 (2003).

30. A.A. Soliman and W. Linert, **Thermochimica Acta, 333**, 67-75 (1999).

31. A.P. Mishra, **J. Indian Chem. Soc. 76,** 35-37 (1999).

32. A. Kriza, M. Voiculescu and A. Nicolae, **Analele Universitatii Bucuresti. Chimie, 11,** 197- 201 (2002).

33. J.K. Nag, D. Das, B.B. De and C. Sinha, **J. Indian Chem. Soc. 75,** 496-498 (1998).

34. M. Hossain, S.K. Chattopadhyay and S. Ghosh, **Polyhedron, 16,** 1793-1802 (1997).

35. M.M. Moustafa, **J. Thermal Anal. 50**, 463-471 (1997).

36. G.G. Mohamed, Nadia E.A. El-Gamel and F.A. Nour El-Dien, **Synth. React. Inorg. Met.- Org. Chem.31,** 347-358 (2001).

37. F.A. Cotton, G. Wilkinson, C.A. Murillo and M. Bochmann, "**Advanced Inorganic Chemistr**y", 6th ed., Wiley, New York, 1999.

38. D.R. Zhu, Y. Song, Y. Xu, Y. Zhang, S.S.S. Raj, H.K. Fun and X.Z. You, **Polyhedron, 19**, 2019- 2025 (2000).

39. R. Prasad, P.P. Thankachan, M.T. Thomas and R. Pathak, **J. Ind. Chem. Soc. 78**, 28-31 (2001).

40. M.S. Masoud, A.M. Hindawy and A.S. Soayed, **Trans. Met. Chem. 16**, 372-376 (1991).

41. N.K. Gaur, R. Sharma and R.S. Sindhu, **J. Ind. Chem. Soc. 78**, 26-27 (2001).

42. M.M. Omar and Gehad G. Mohamed, **Spectrochimica Acta, Part A, 61,** 929-936 (2005).

43. N. Mondal, D.K. Dey, S. Mitra and K.M. Abdul Malik, **Polyhedron, 19**, 2707-2711 (2000).

44. J. Kohout, M. Hvastijova, J. Kozisek, J.G. Diaz, M. Valko, L. Jager and I. Svoboda, **Inorg Chim. Acta 287**,186-192 (1999).

45. A. Bury, A.E. Underhill, D.R. Kemp, N.J. O'Shea, J.P. Smith, P.S. Gomm and F. Hallway, **Inorg. Chim.Acta, 138**, 85-89 (1987).

46. N.R.S. Kumar, M. Nethiji and K.C. Patil, **Polyhedron, 10,** 365-371 (1991).

47. J. Manonmani, R. Thirumurugan, M. Kandaswamy, M. Kuppayee, S.S.S. Raj, M.N. Ponnuswamy, G. Shan-mugam and H.K. Fun, **Polyhedron, 19**, 2011-2018 (2000).

48. J. Sanmartin, M.R. Bermejo, A.M.G. Deibe, M. Maneiro, C. Lage and A.J.C. Filho, **Polyhedron, 19**, 185-192(2000).

49. V.P. Krzyminiewska, H. Litkowska and W.R. Paryzek, **Monatshefte Fur Chemie, 130**, 243-247 (1999).

50. K.Bertoncello, G.D. Fallon, K.S. Murray and E.R.T. Tiekink, **Inorg. Chem. 30**, 3562 (1991).

51. , "**Microbiology in Clinical Practice**", Wright PSG, Bristol, London, Boston, 1982.

52. E. Jawetz, J.L. Melnick and E.A. Adelberg, "**Review of Medical Microbiology**", Lang Medical Publications, Los Angeles, California, 16th ed., 1979.

53. A.M.S. El-Sharief, M.S. Ammar, Y.A. Ammar and M.E. Zak, **Ind. J. Chem. 22B**, 700-704 (1983).

54. A.M.S. El-Sharief, M.S. Ammar and Y.A. Mohammed, **Egypt. J. Chem. 27,** 535-546 (1984).